

# Optimization of Aeration Variables in a commercial large-scale flat-sheet MBR operated with Slug Bubbling

**Bing Wang<sup>a,b</sup>, Kaisong Zhang<sup>a,b\*</sup>, Robert W. Field<sup>c</sup>**

<sup>a</sup> *Key Laboratory of Urban Pollutant Conversion, Institute of Urban Environment, Chinese Academy of Sciences, Xiamen 361021, China*

<sup>b</sup> *University of Chinese Academy of Sciences, Beijing 100049, China*

<sup>c</sup> *Department of Engineering Science, University of Oxford, Oxford OX1 3PJ, UK*

\* Corresponding author: KS Zhang, [kszhang@iue.ac.cn](mailto:kszhang@iue.ac.cn)

## **Abstract**

It has been established that slug bubbling is an effective strategy to control fouling in flat sheet MBRs (FSMBR). Following prior work that ascertained optimal values of plate thickness and channel gaps, the focus here is on optimizing aerator spacing for operation under a range of aeration rates. The overall objective is to enhance fouling control of commercial-scale FSMBRs through optimization of the bubble distribution and the intensity of the induced shear stress. Three-dimensional Computational Fluid Dynamics (CFD) simulation was used to predict the aeration process of bubble coalescence, development, split and distribution into channels between every membrane pair. The bubble features and behavior were analyzed and compared with experimental measurements and substantial agreement was obtained. The aeration inlet conditions, including aerator spacing, were varied to control the slug bubbling process. The combination of aeration inlet velocity at 11 m/s and aerator spacing of 104 mm was verified to be an optimal condition, which would give a combination of uniform distribution of slug bubbles between the plates, high induced shear stress at the membrane surface and an economic air consumption. The aeration consumption for 100 sheets of membranes would be reduced by 47% compared to the conventional industrial norm.

## **Key Words**

Flat sheet MBR; slug bubbling; CFD; air consumption; fouling control.

# 1. Introduction

Flat sheet MBR (FSMBR) are a highly compatible and effective device applied widely in waste water treatment and reclamation applications. However, the pressure-driven membrane filtration performance is significantly influenced by membrane fouling, the amelioration of which results in higher aeration cost and occasional membrane replacement expenditure. This reduces its attractiveness in comparison with the traditional activated sludge process (CASP) [1-3]. Therefore, various aeration regimes have been developed to enhance the hydrodynamic effect in FSMBR [4-7]

One of the pioneering studies on the effect of slug bubbling was carried out by Cui et al., which showed that the slug bubbles could strengthen surface shear, give effective control of concentration polarization and so ameliorate membrane fouling [1, 8, 9]. Early studies from 2006 by Zhang et al. indicated the attractiveness of applying periodic slug bubbling to FSMBRs; it generated a more effective and economic way to enhance the mass transfer coefficient and induce high wall shear stress while consuming only a modest amount of air [10, 11]. It was established that slug bubble size in flat sheet MBR modules is a critical parameter because it has a major influence on surface sheer stress of the membranes [12]. Previous electrochemical experiments had showed that shear stress from over 60 mL slug bubble could produce excellent spanwise sheer stress of more than 1.0 Pa on the flat membrane [12]. Having established that the hydrodynamic effect introduced by slug bubbles is more effective and economic in fouling amelioration between two membranes in flat sheet MBRs (FSMBR) than conventional bubbling, our recent work has been focused on its implementation in a commercial-scale FSMBR [13, 14], consisting of 100 membranes of the size normally used in industry. Recently a novel slug bubble production method has been developed through a two-stage

process of bubble coalescence above the aerator followed by bubble splitting to ‘feed’ a number of channels [13]. This has proven to be fundamental to the implementation of slug bubbling hydrodynamics to large-scale FSMBRs [13]. In our recent work it has been established that the combination of membrane plate thickness of 5mm and a channel gap of 6mm gave a uniform distribution of slug bubbles and high shear stress in all of the channels [14]. The current paper builds upon these works by considering a furthermore study on controlling this novel aeration process, through the variation of bubbling flow rates and aerator spacing. To aid industrial application an optimization method is proposed herein to cover a wide range of air flow rates, such as those used by Oxiamembrane Co., Ltd, Xiamen, China

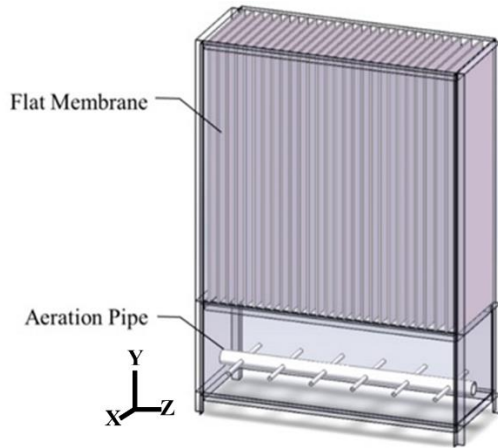
As noted previously Computational Fluid Dynamics (CFD) is a powerful tool for understanding the bubbling regime and two-phase hydrodynamics by characterizing the flow conditions through solving the mathematical equations [14-16]. Such simulations can remarkably reduce time and cost compared to repeated experiments and CFD simulations have been widely applied to membrane processes, especially to MBRs, to predict the hydrodynamic characteristics including shear stress distribution at a membrane surface and turbulence [17-26]. For FSMBR, Wei et al. studied the slug bubbling between two membranes in various conditions by CFD simulation and image analyses [12]. Later Wang et al. built a novel slug bubbling process through CFD simulation for a large-scale FSMBR with 100 membranes [13]. Subsequently an optimal condition of membrane plate thickness and channel gap was reported; again based on a combination of both CFD calculations and image analyses [14].

In general the studies on FSMBR still lack research data comparable to that available for hollow fiber MBRs. in particular there was few studies on large bubble hydrodynamics in commercial-scale flat sheet MBRs. Therefore, the overall objective of this work is to theoretically and experimentally set up a hydrodynamic

optimization method for commercial-scale flat sheet MBRs based on our novel coalescent bubbling process. The hydrodynamic features were quantified to determine the coalescent bubble characteristics, the optimization for slug bubble effect inside channels, and shear stress distribution on all membrane walls under different operating conditions. This was accomplished here by conducting CFD simulations and experimental measurements to obtain detailed information on the control process of slug bubbling. The distribution of bubbles formed from the splitting of one large-sized coalescent bubble was studied through optimization of aerator spacing for various aeration rates. Special attention was paid to the induced shear stress on membrane walls which could directly influence the fouling control. Moreover, aeration consumption was calculated and the optimal conditions for an economic air flow demand was determined.

## 2. Methods

The Methods were developed from those used previously [14]. Details of the experimental method are given in Supplementary Material, section S1. In the present work the channel gap was fixed at 6 mm and the plate thickness at 7 mm. Previously the aeration velocity at the nozzle had been fixed at 12 m/s but herein it is varied between 5 ~ 17 m/s. A schematic of the layout is given in Fig S0. The central pipe of the aerator is orthogonal to the membrane plates and it supplies air to a series of side pipes. The spacing between nozzles in the side pipes is 10 mm. The frequency of slug bubbling was maintained at 1 Hz. Fig. S1 provides a schematic diagram of the experimental setup for slug bubbling.



Section S2 of Supplementary Materials gives details for the CFD Simulation Method including the physical model, the meshing, the governing equations and the numerical method used. Figure S2 shows an example of a typical mesh.

### 3. Results and Discussion

#### 3.1 Variation of air velocity

##### 3.1.1 Coalescent bubble development comparison

In the zone below the membrane, a large-sized bubble can be generated from single bubbles through side-by-side coalescence as shown in a previous study [12]. Here, this process is compared in Fig. 3 for two aeration rates of 5m/s and 17m/s using CFD predictions and experimental images. The bubble sizes in three directions were measured and plotted as function of bubble position height (height from bubble to nozzles) in Fig. 4. Both CFD results and experiment images (Fig. 3) showed that during bubble coalescence process, single bubbles were already coalesced into one bubble before they detached from the nozzles in the case of 17m/s aeration rate, whilst the single bubble outlines were still clear after they detached the pipe when the rate was 5m/s. Fig. 4 also shows that the bubble dimensions for all directions were similar for the two cases before coalescence into one large-sized bubble.

However at the height of 35mm, there was a sharp jump of 5-fold in size for the X-direction at 17m/s compared with that found for 5m/s. This implies the bubbles could coalesce more readily and earlier at high aeration rates. Although single bubbles successfully merged into one bubble for the 5m/s case, one can envisage that incompletely coalescence may happen with lower aeration rates.

After merger of the bubbles from the nozzles, the coalescent bubbles developed and expanded into large-sized bubbles. Fig. 4 indicates that bubbles grew faster at higher aeration rate. Additionally, at the height of 55 mm, the coalescent bubble had totally detached from the aeration pipe and expanded faster for the case of 17 m/s. By varying aeration rates, bubble size contacting the base of membranes could be controlled; this directly influences the slug bubble volume and induced hydrodynamic effect on the membranes. Both CFD predictions and experimental data showed very similar trends, indicating that a good understanding of large-sized bubble formation had been achieved. Furthermore it was confirmed that this novel bubbling method could be operated over a wide aeration rate range (from 5m/s to 17m/s). This was confirmed by studying the bubbling process at other five aeration velocities (i.e., 7m/s, 9m/s, 11m/s, 13m/s and 15m/s). Again there was good agreement between CFD simulation and experiments.

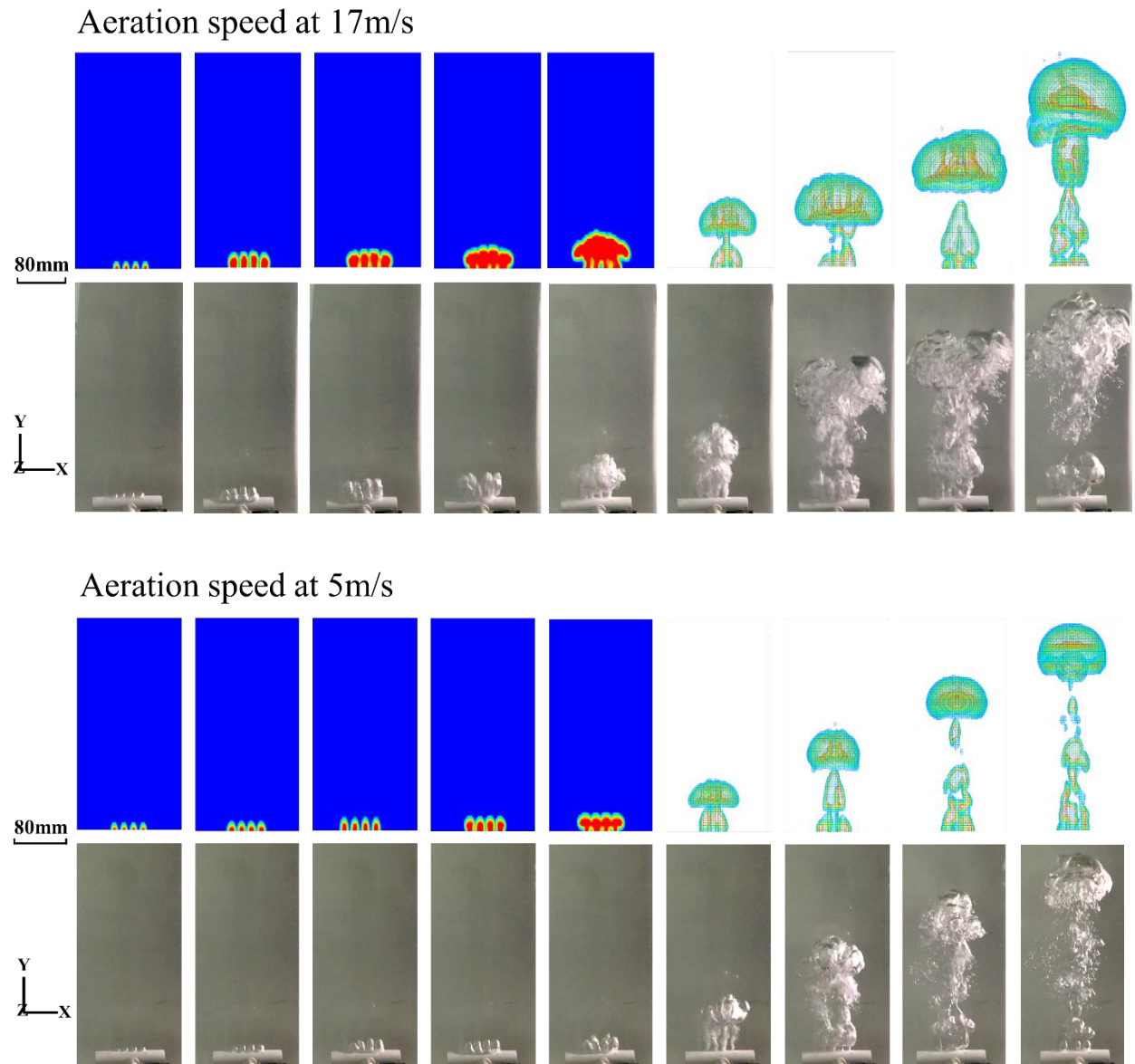


Fig. 3 CFD and experiment observations on bubble coalescence and development into large-sized bubble below the base of the membrane plates for rates of 17m/s and 5m/s.



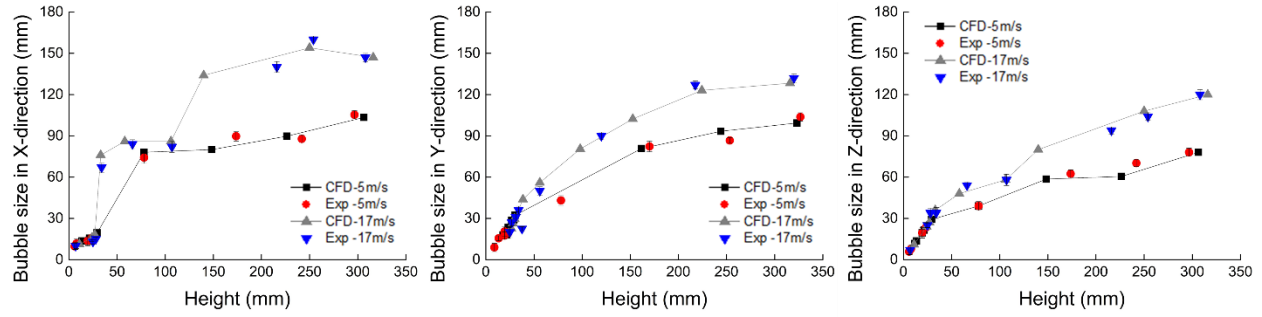


Fig. 4 Bubble size development: a comparison of CFD results with experimental data.

### 3.1.2 Bubble size comparison

In Fig. 5, the three-dimensional bubble shape at the position of 280mm height is shown. At this location the bubble is stable and no fragmentation has happened. The large-sized coalescent bubble could be produced at all aeration rates (5m/s to 17m/s) and its size increased in all dimensions as the aeration rate increased. Bubbles from CFD simulation were good agreement with the corresponding experimental images.

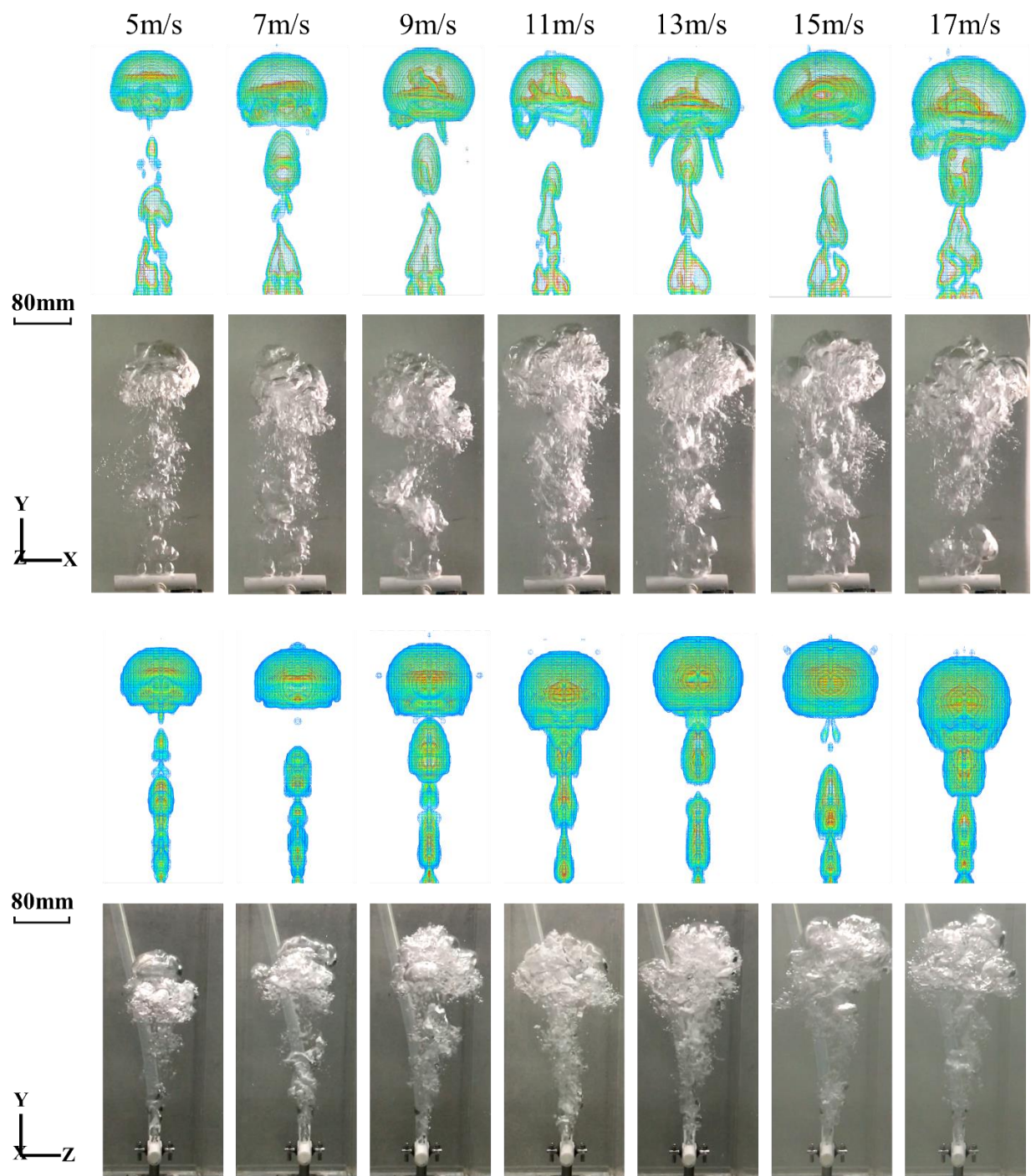
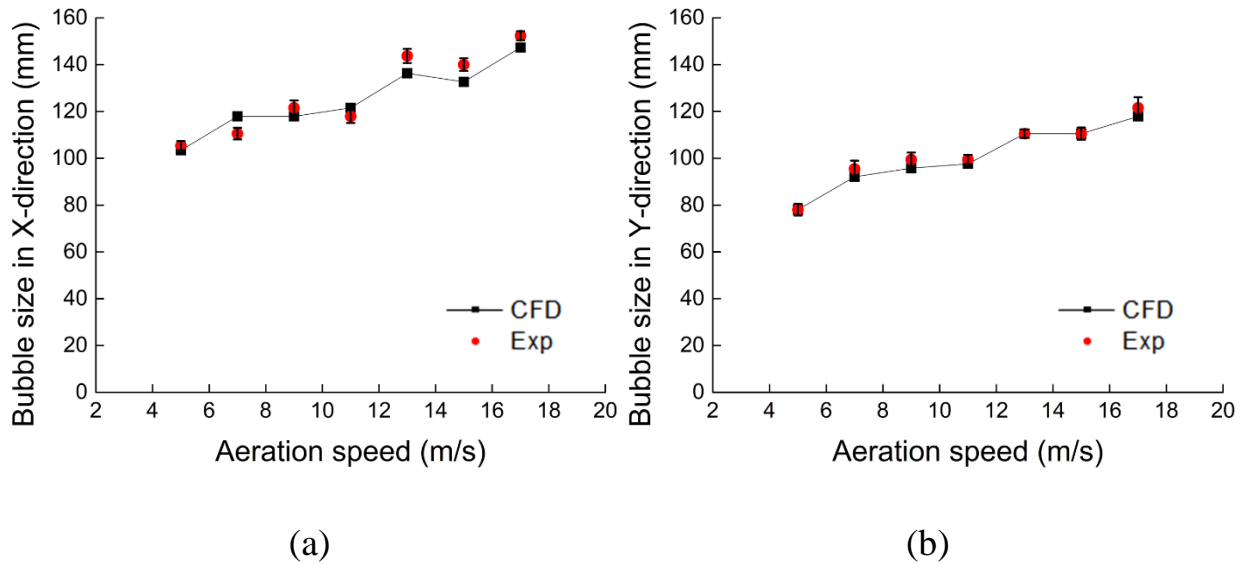
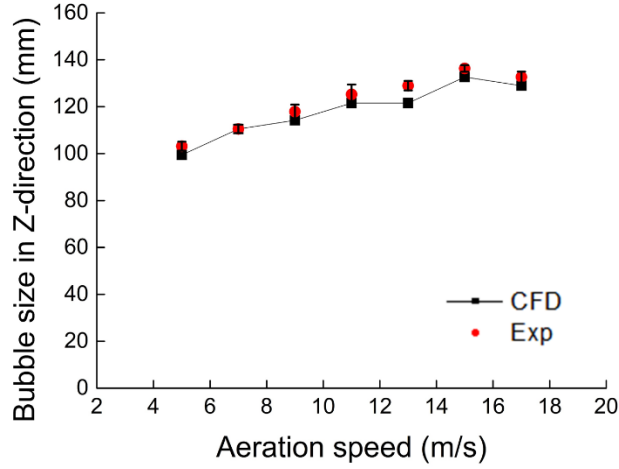


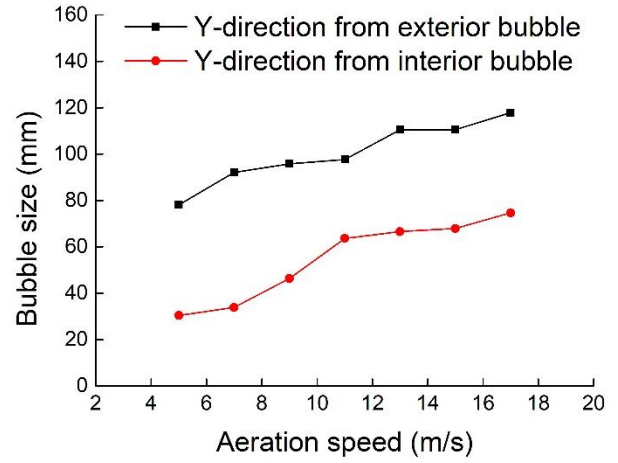
Fig. 5 Contour images of stable bubble at seven different aeration rates from CFD simulation and experiment results.

Further validation was made by directly comparing the bubble dimensions at different air-velocities. In Fig. 6 (a)-(c), a plot of bubble size is provided for both CFD simulation and experimental measurements as a function of air velocity. The typical standard deviation was found to be small ( $<5\%$ ), indicating that the results were highly reproducible. Significant agreement can be observed between the experimental and computational results which validates the CFD modeling approach as one which can give appropriate predictions of the hydrodynamic features. It showed that from low to high air velocities the bubble size increased by nearly 43 mm in X- and Y-directions but more slowly by 29 mm in the Z-direction. The size of coalescent bubble was strongly dependent on the aeration rates, particularly below 11 m/s air velocity and is discussed in more detail in the next section.





(c)



(d)

Fig. 6 (a)-(c): Bubble size measurements comparison of CFD results with experimental data; (d) measurement from CFD results for the air domain at interior top region.

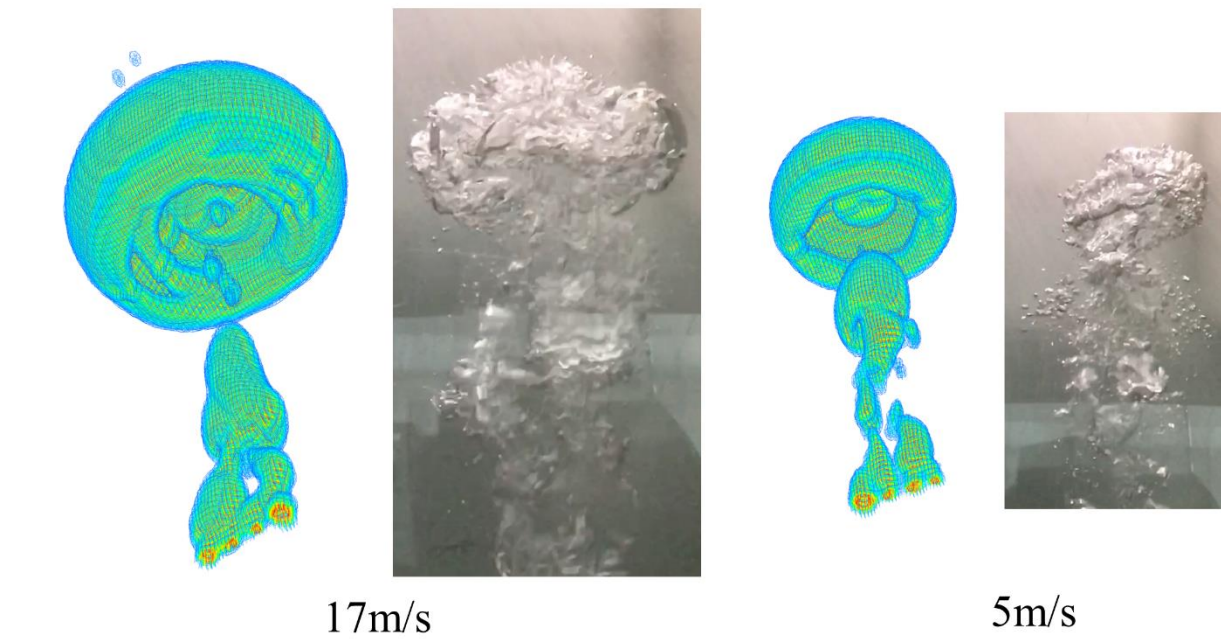


Fig. 7 Bubble inside in 45° bottom view at aeration rate of 5m/s and 17m/s

## 3.2 Variation of aerator spacing

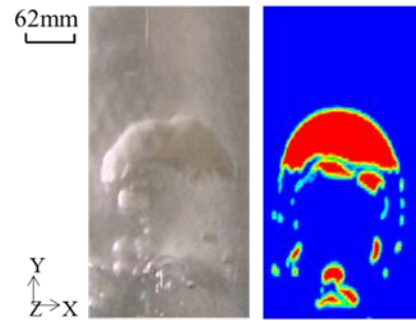
### 3.2.1 Bubble lateral spread

The coalescent bubbles could cover an extensive range of membrane sheets because of their extensive lateral spread. These large-sized bubbles split upon contacting the base of the membranes and bubbles are distributed into different channels. The experimental image of bubbles in a channel between a membrane and a sheet of transparent plexiglass is shown in Fig. 9 (a). The experimental image showed a slug bubble that has a large spherical cap shape followed by several small bubbles in the wake and, as shown, this was similar to the CFD simulation.

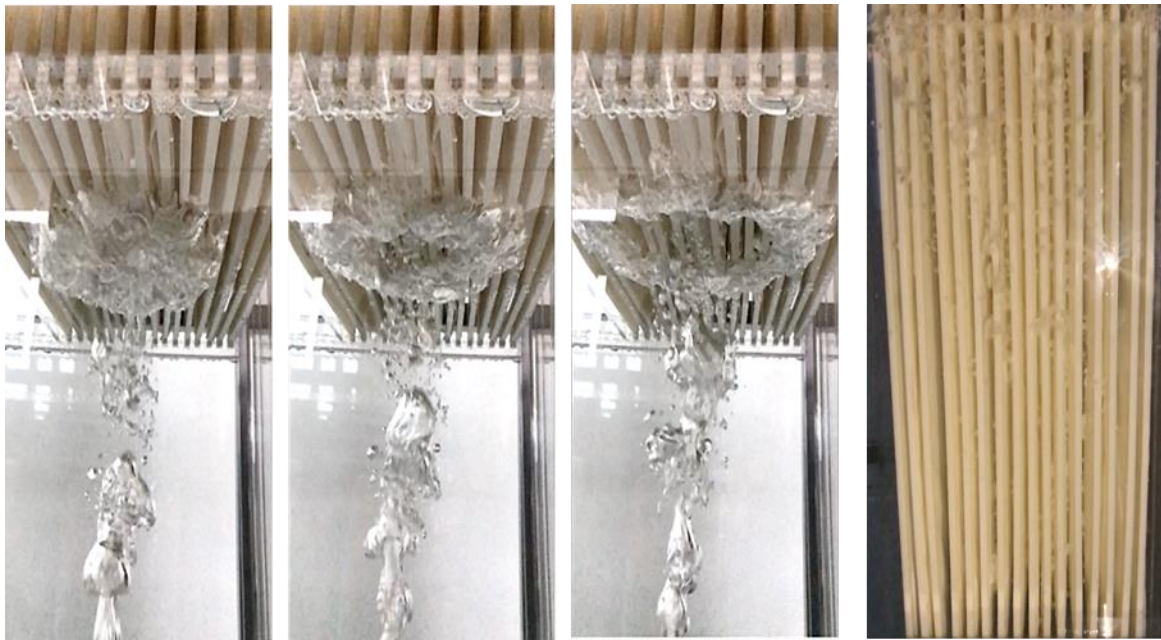
From the plot in Fig. 7 the bubble size was estimated to be around 100mm in Z-direction. Without lateral spreading that occurs on contact with the plates, the single bubble would have covered just 9 channels but it was found to cover 27 channels as shown in Fig. 9 (c).

The side view of channels shows which channels receive bubbles but a front view of the bubbles – views towards the face of the membrane surfaces – is required to estimate size and shear stress. With a spacing of 286 mm, the bubbles distributed to channels 6 to 10 were much smaller, with small shear stresses of *circa* 0.35 Pa, than those for channels 11-14. As higher shear stress is necessary to control potential fouling, large-scale FSMBR units need to be optimized not only for laterally spread and also in terms of the ability of the bubbles to generate higher shear stress within all channels. This matter is considered further in the next section.





(a)



View from below plates

Side view

(b)

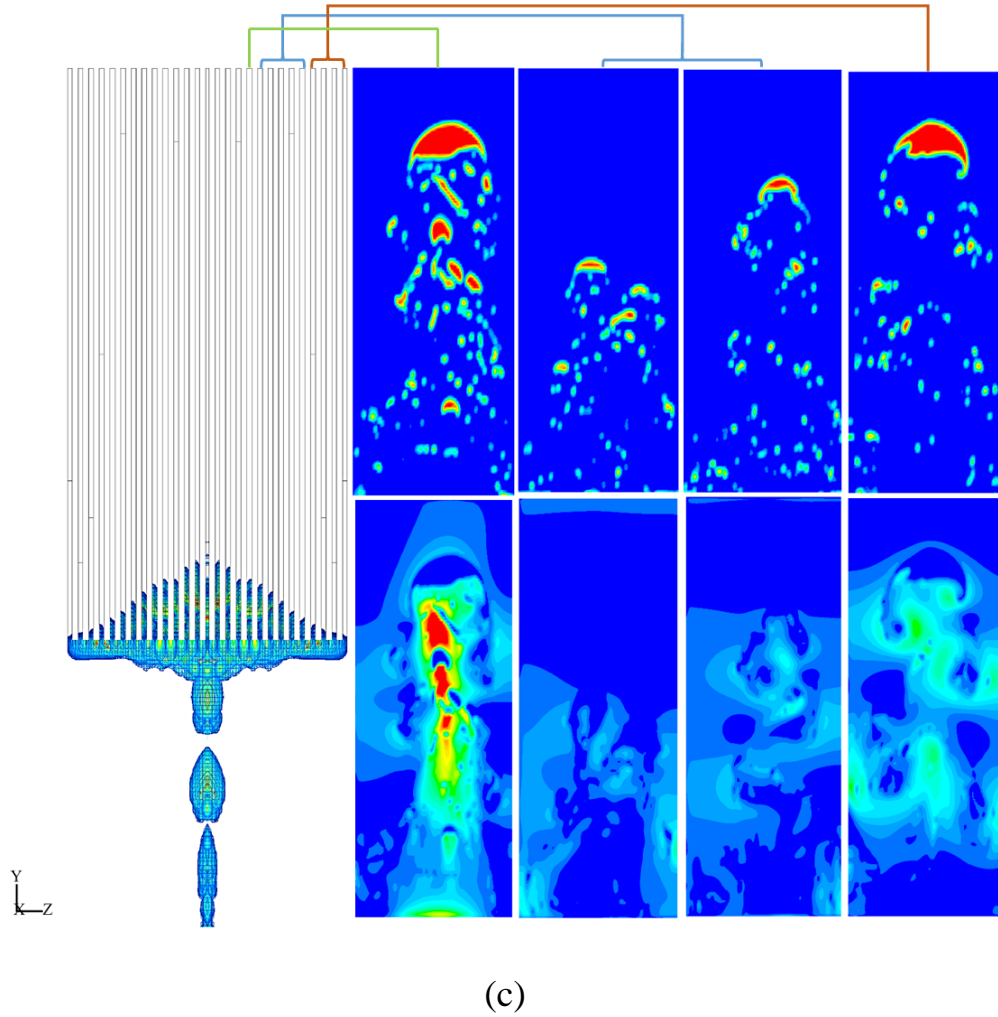


Fig. 9 (a) Front view of CFD result and experiment image taken between a membrane and a sheet of transparent plexiglass – air velocity is 14m/s [13]; (b) Views of large-sized bubble being distributed between membranes from below plates and the side [12]; (c) Bubble split and distribution at aeration rate of 15 m/s with channel coverage of 27, with aerator interval of 286 mm.

### 3.2.2 Optimization of channel coverage

The lateral spread of bubbles can be controlled by adjusting the aeration pipe spacing. According to the considerations in section 3.1, quality channel coverage

was calculated to be 9. Fig. 10 illustrates the case for an aeration velocity of 15 m/s with coverage by one bubble being 10 channels. This equates to an aerator spacing of 130 mm (channel width is 6mm and membrane width is 7mm).

For the same fixed aeration rate of 15 m/s, a range of aerator designs were investigated. All produced one large-sized coalescent bubble as shown in Fig. 10.

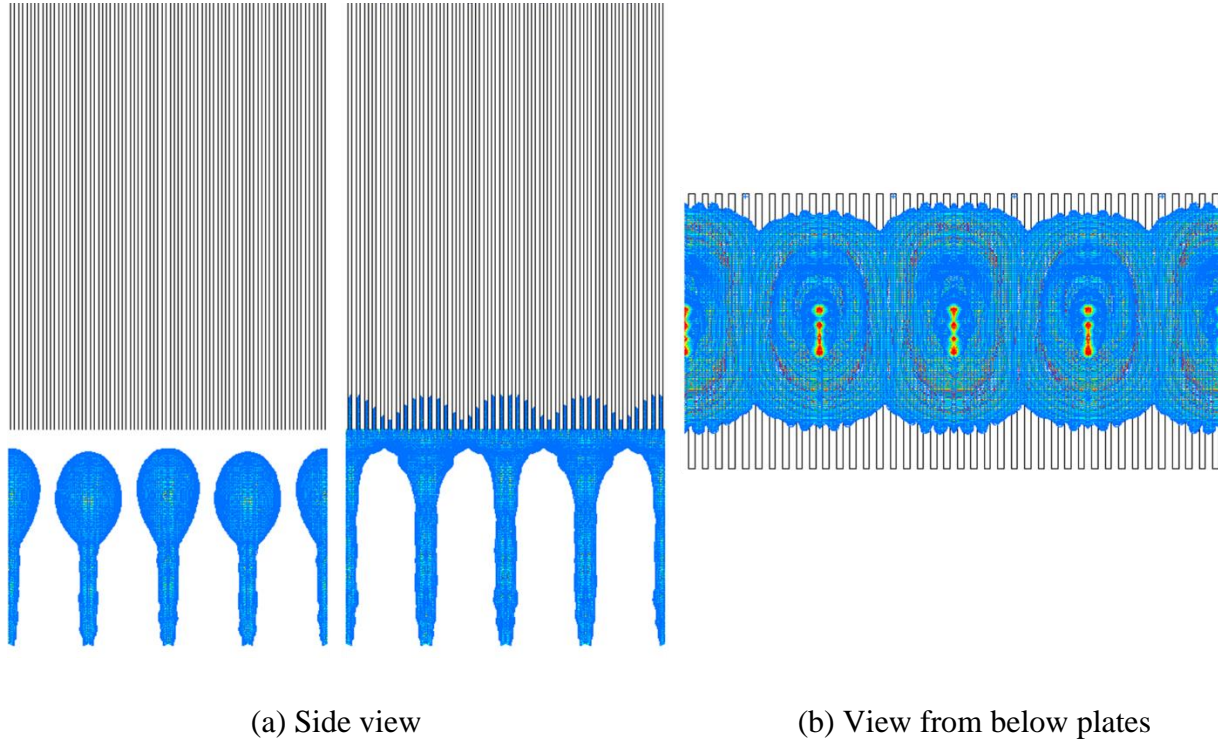


Fig. 10 Views of large-sized bubbles being distributed between membranes at aeration rate of 15m/s: (a) side view; (b) view from below plates.

As the pipe spacing decreased from 286 mm to 260 mm. the size of split bubble in channels 6 - 10 (see Fig. 9 (c)) increased dramatically (see Fig. 11 for channels 7 - 10. The shear stress also increased but it was still relatively small with most of regions below 1Pa on the membrane surface in channels 7 ~ 8. As the aerator spacing decreased to 208 mm with coverage of 16 channels, the bubble size slightly



increased in channel 7 but it significantly decreased in the last channel. Shear stress was enhanced in the channel 7 but weakened in the last one. Although the bubble distribution and shear stress were somehow improved compared to the previous condition (Fig. 9 (c)), the bubble size and shear stress in the last few channels was not stable. Further improvements were made by a small adjustment to the 18mm aerator interval so that it gave 14 rather than 16 channel coverage (see Fig.11). Not only was bubble size more uniform in the last few channels but the shear stresses were enhanced to be more than 1.75 Pa for all the channels.

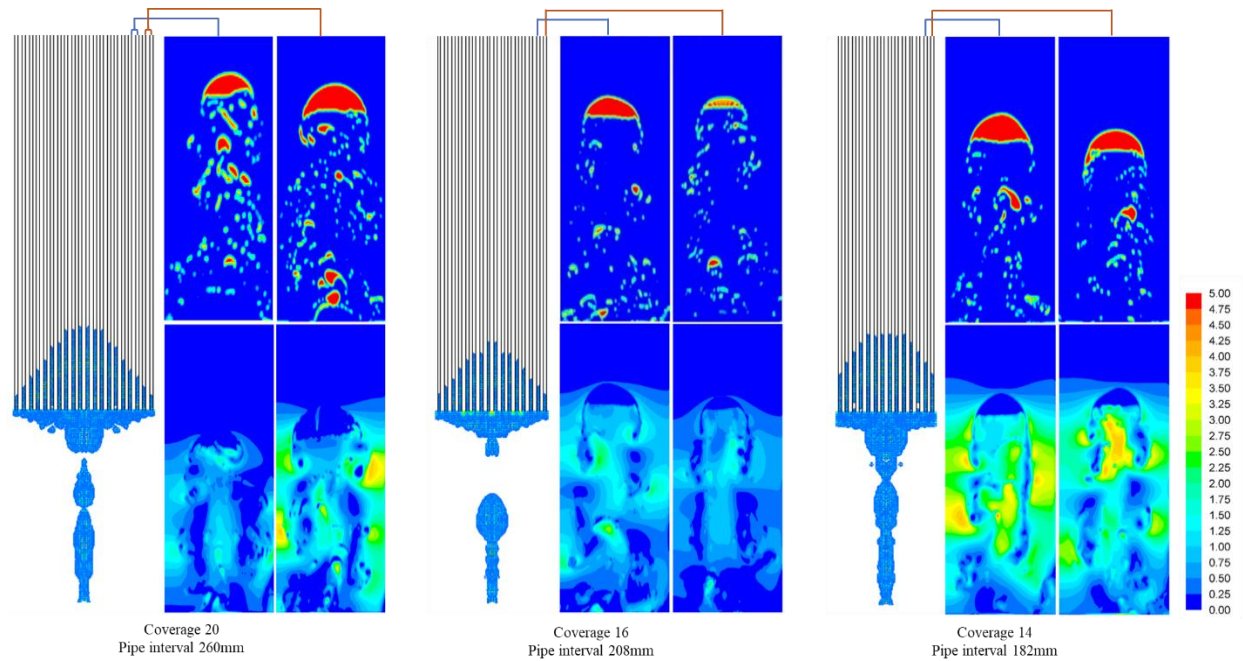


Fig. 11 Contours of bubble distribution and shear stress with channel coverage optimization at air velocity of 15m/s.

### 3.3 Optimized effect

Aerator spacing was investigated for the other six aeration rates (i.e., 5m/s, 7m/s, 9m/s, 11m/s, 13m/s and 17m/s). As the pipe interval decreases the total number of aerators increase which would result in higher air consumption and energy cost. As the optimization should be based on a rational upper limit to the total air consumption only those conditions utilizing less than 1000 L/min (assumed 100 membranes) were considered. This limit was based on an estimate of the average used in traditional industrial MBRs. Only those arrangements above the line in Table 2 were considered further. Overall 49 CFD simulations were carried out by varying channel coverage (from 28 and to 2) for all aeration velocities shown in Table 2, with aerator spacing decreasing from 364 mm to 52 mm and total number of aerators increasing from 8 to 50.

Table 2 Total Flow Rate in FSMBR (L/min)

Channel Coverage	Pipe Spacing (mm)	Number of Aerators	Aeration Usage (L/min)						
			5	7	9	11	13	15	17
28	364	8	121	169	217	265	314	362	410
20	260	10	151	211	271	332	392	452	513
16	208	12	181	253	326	398	470	543	615
14	182	14	211	296	380	464	549	633	718
12	156	16	241	338	434	531	627	724	820
10	130	20	302	422	543	664	784	905	1025
8	104	26	392	549	706	863	1019	1176	1333
6	78	34	513	718	923	1128	1333	1538	1743
4	52	50	754	1056	1357	1659	1960	2262	2564
2	26	102	1538	2153	2769	3384	3999	4614	5230

The optimal cases for air velocity range (5-17 m/s) of half system (because of symmetrical condition) were presented in Fig. 12, which could produce slug bubbles

with uniform distribution and high shear stress. Due to different aeration rates and coalescent bubble size, the optimized channel coverage were different. Shear stress was found to be over 2 Pa for more than 80% regions especially the wake region on each membrane wall. From aeration rate 11 m/s to 9 m/s, the channel coverage decreased by 3 in half system (6 channels in whole system), which was the most reduction. From speed 11m/s to 13m/s, channels coverage was the same, whilst, it was reduced by 1 in half system (2 channels in whole system) at aeration rate 13m/s to 15m/s. For 17m/s aeration rate two more channels could be covered than that of 11m/s Figs. 7 and 8). The channel coverage increased slowly in the air velocity range of 13 ~ 17 m/s.

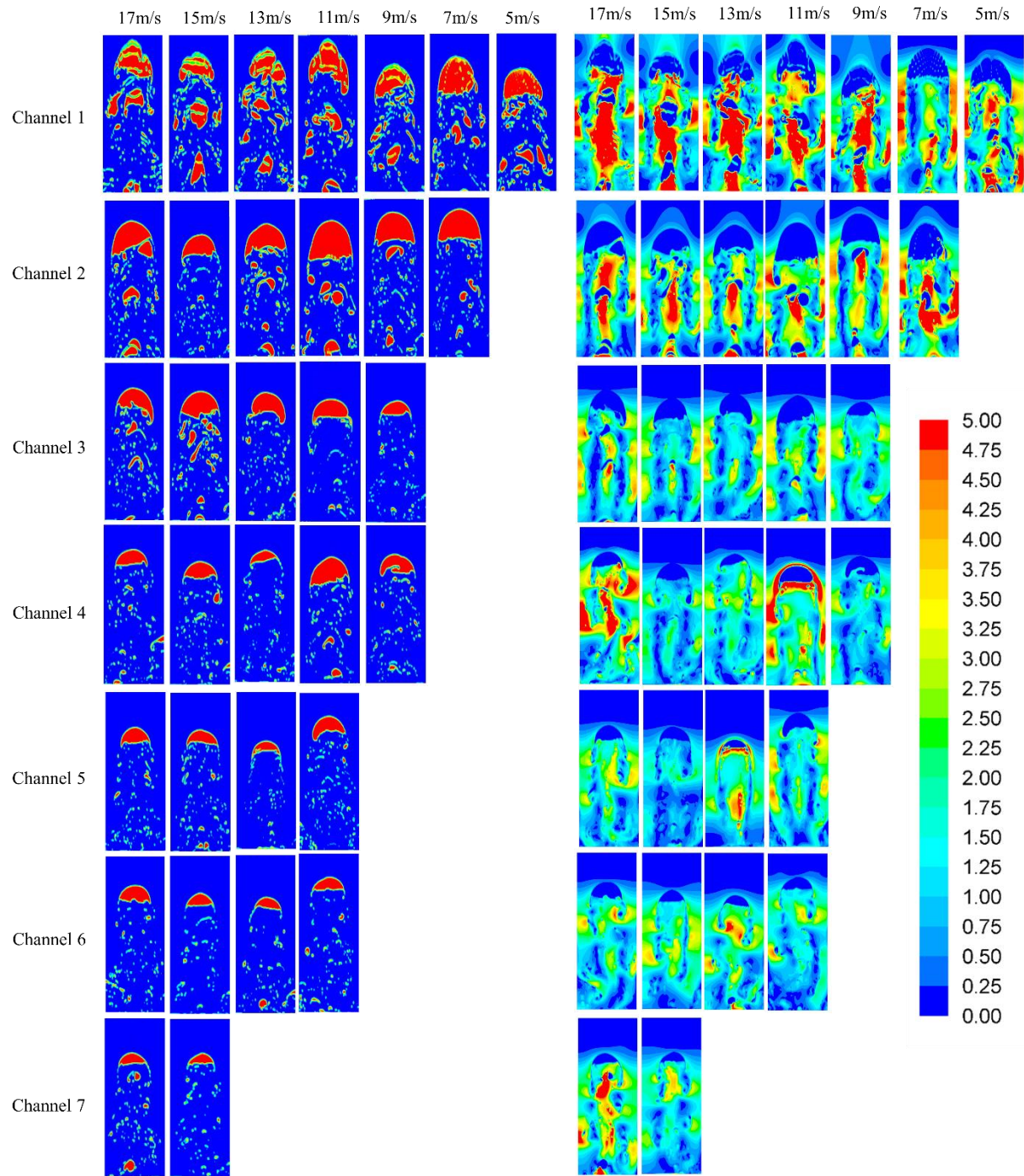


Fig. 12 Contours of bubble distribution and shear stress in optimal channel coverage cases for aeration rates range from 5m/s to 17m/s.

With aeration rate increasing from 11m/s to 17m/s, the shear stress increased, in general, for the first three channels; but it was very close for the other channels. As one can see in Fig. 13, for example, the average shear stress at 15m/s was 1.1 times than that at 11m/s, but it was close for the channel 4-7. The shear stress was more uniform as the aeration rates decreased, since the shear stress in central channels decreased more than the other channels. In determining the optimal aeration rate it is suggested that attention should not be given to the shear stress in the central channels, where it is strong, but attention should be focused on the uniformity of average shear stress across the different channels.

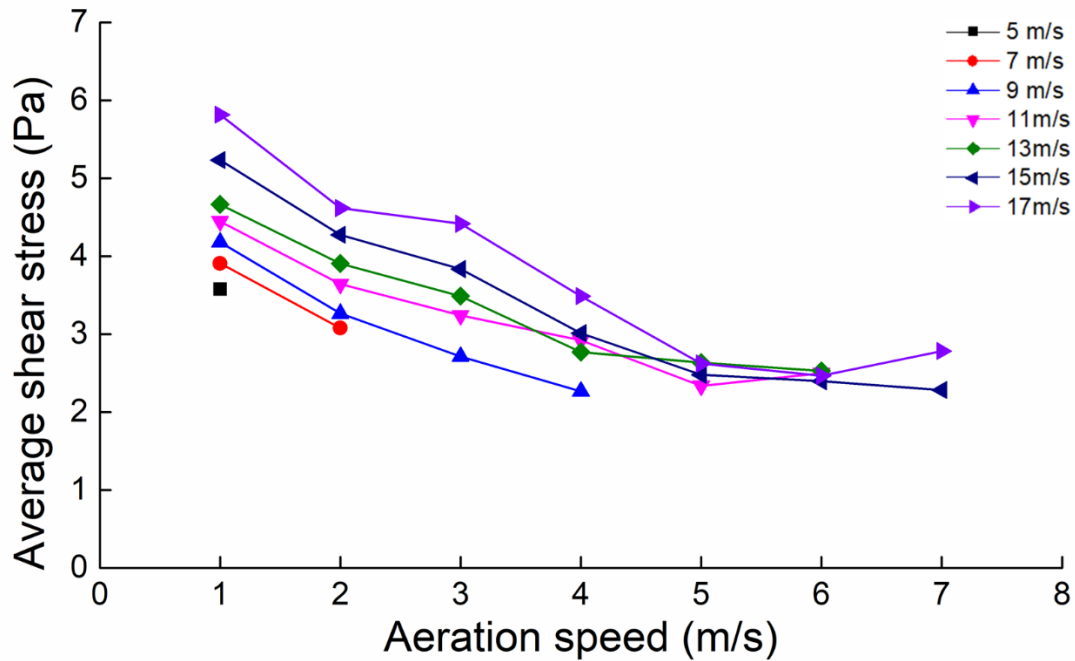


Fig. 13 Average shear stress in channels for half system at the aeration rate range of 5m/s to 17m/s.



### 3.4 Energy Consumption

Based on the optimization, the number of channels effectively covered by one coalescent bubble could be determined, and the number of aerators could be calculated by assuming that the total number of membrane plates was 100. As shown in Fig. 15 the channel coverage increased from 2 to 12 as the aeration speeds increasing from 5m/s to 11m/s, and only very modestly thereafter. The number of required aerators decreased rapidly from 50 to 28 at aeration speed of 5m/s to 9m/s, and then decreased slowly from 28 to 12 as the air velocity increased from 9m/s to 11m/s. As many more aerators would be needed in the low air velocity range of 5m/s to 7m/s, this would not be a realistic choice for water treatment applications. So for the aerator containing 4 nozzles, the air velocity should be above 9 m/s with larger velocities between 11 m/s and 17 m/s producing more effective slug bubbles.

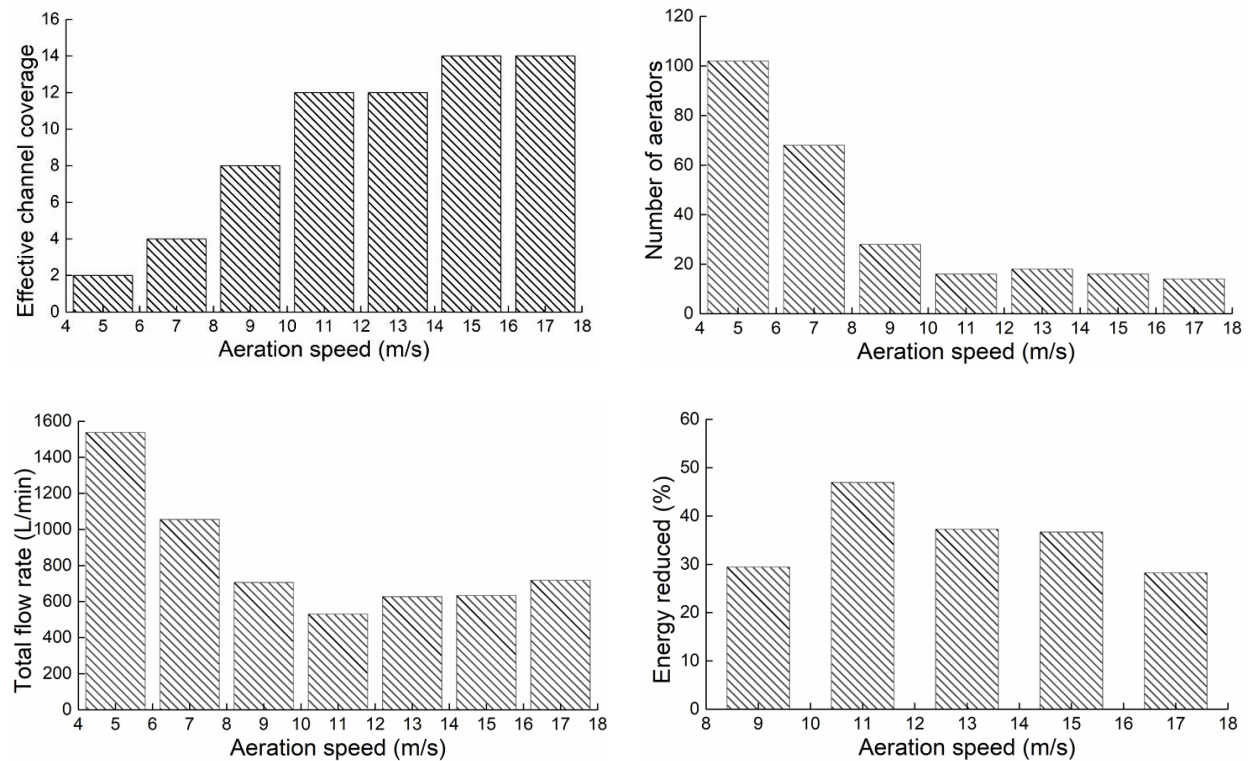


Fig. 15 Optimized parameters in this novel bubbling approach and corresponding energy reduction.

As shown in Fig.15 the total aeration consumption sharply decreased as aeration speed increased from 5m/s to 11m/s and then slightly increased between 11m/s and 17m/s. This established the optimal aeration speed to be 11m/s as it not only provides effective slug bubbles it is also the most energy saving case. Compared to a normal industrial consumption (10 L/min/membrane sheet) the air flow rate reduction percentage was found to be 24% to 47% in the aeration speed range of 9m/s to 17m/s (Fig. 15).

## 4. Conclusion

From a numerical CFD study and corresponding experiments in a large-scale flat sheet MBR unit, hydrodynamic optimization of the coalescent slug bubbling process was undertaken. Bubble growth behavior, its coverage of the membrane channels and the shear stress on membrane walls were evaluated and compared across a range of aeration speeds 5 m/s ~ 17 m/s. The predicted shear stress profiles were compared under different operating conditions. The resultant bubble sizes varied with aeration velocity and the simulations agreed well with experimental measurements. The shear stress distribution could be enhanced, especially for the off-centre membranes, by decreasing the aerator spacing (and thus the number of channels covered). The effective channel coverage varied with aeration speed and it increased from 2 to 14 as the aeration velocity increased from 5m/s to 17m/s; higher velocities resulted in a more uniform distribution of shear stress on the membrane walls.

Higher shear stress is caused by two regions, the wake region and the liquid film region. Turbulence was enhanced more in the wake region by increasing the aeration speed. With optimized spacing the average shear stress was above 1.5 Pa

at all aeration velocities and found to increase with the aeration velocity. The bubbles swept across more than 70% of the membrane width in all channels, and over 80% of the membrane area experienced shear stresses above 2 Pa. There were energy cost savings for a wide range of aeration velocities from 9 m/s to 17 m/s, with the maximum saving being 47% at an aeration condition of 11 m/s.

The novel process of slug bubbling provides an economic advantage which is particularly important in waste water applications. Besides the reduced energy costs, the enhanced shear stress will limit fouling. Overall it is expected that the results of this work will lead to optimization of the slug bubbling process in large-scale commercial FSMBRs.

## Acknowledgements

This work was supported through the grants from the Bureau Frontier Sciences and Education (QYZDB-SSW-DQC044), the Bureau of International Cooperation (132C35KYSB20160018), Chinese Academy of Sciences and Oxiamembrane Co., Ltd, Xiamen, China. We would also like to thank Dr. Olusegun Abass and Mr. Xingbiao Chen for their help, comments, and assistance.

## References

- [1] Z.F. Cui, Experimental investigation on enhancement of crossflow ultrafiltration with air sparging, in: R. Paterson (Ed.), *Effective Membrane Processes—New Perspectives*, Mechanical Engineering Publications Ltd, London, 1993, 237–245.
- [2] Pawel Krzeminski, Lance Leverette, Simos Malamis, Evina Katsou. Membrane bioreactors - A review on recent developments in energy reduction, fouling control, novel configurations, LCA and market prospects. *J. Membrane. Sci.* 527 (2017) 207-227.
- [3] Z. F. Cui, S. Chang, A. Fane, The use of gas bubbling to enhance membrane processes, *J. Membrane. Sci.* 221 (2003) 1-35.
- [4] Q.Y. Li, Z.F. Cui, D.S. Pepper, Effect of bubble size and frequency on the permeate flux of gas sparged ultrafiltration with tubular membranes, *Chem. Eng. J.* 67 (1997) 71–75.
- [5] R. W. Field, K. S. Zhang, Z. F. Cui, B. K. Hwang. Flat sheet MBRs: analysis of TMP rise and surface mass transfer coefficient. *Desalin. Water. Treat.* 35 (2011) 82-91.
- [6] L De Temmerman, T Maere, H Temmink, A Zwijnenburg, I Nopens. The effect of fine bubble aeration intensity on membrane bioreactor sludge characteristics and fouling. *Water Res.* 2015; 76: 99-109.
- [7] E. Braak, M. Alliet, S. Schetrite, C. Albasi, Aeration and hydrodynamics in submerged membrane



bioreactors, *J. Membrane. Sci.* 379 (2011) 1-18.

[8] R. Ghosh, Z.F. Cui, Mass transfer in gas-sparged ultrafiltration: upward slug flow in tubular membranes, *J. Membrane. Sci.* 162 (1-2) (1999) 91-102.

[9] K. S. Zhang K., R.W. Field, Z.F. Cui. Measurement of the mass transfer coefficients in submerged flat sheet membrane systems. The conference of the European Membrane Society, September 24-28, 2006.

[10] K. S. Zhang, Z.F. Cui, R. W. Field. Effect of bubble size and frequency on mass transfer in flat sheet MBR. *J. Membrane. Sci.* 332 (2009) 30-37.

[11] K. S. Zhang, P. Wei, M. Yao, R. W. Field, Z. F. Cui, Effect of the bubbling regimes on the performance and energy cost of flat sheet MBRs. *Desalination.* 283 (2011) 221-226.

[12] P Wei, K S Zhang, W Gao, L Kong, R W Field. CFD modeling of hydrodynamic characteristics of slug bubble flow in a flat sheet membrane bioreactor. *J. Membrane. Sci.* 445 (2013) 15-24.

[13] B. Wang, K. S. Zhang, R. W. Field. Novel aeration of a large-scale flat sheet MBR: a CFD and experimental investigation. *AIChE J.* 64 (2018) 2721-2736.

[14] B. Wang, K. S. Zhang, R. W. Field. Slug bubbling in flat sheet MBRs: Hydrodynamic optimization of membrane design variables through computational and experimental studies. *J. Membrane. Sci.* 548 (2018) 165-175.

[15] Xie F, Liu J. CFD and experimental studies on the hydrodynamic performance of submerged flat-sheet membrane bioreactor equipped with micro-channel turbulence promoters. *Chem. Eng. Process.* 2016; 99: 72-79.

[16] G. A. Fimbres-Weihs. D.E.Wiley. Review of 3D CFD modeling of flow and mass transfer in narrow spacer-filled channels in membrane modules. 49 (7) (2010) 759-781.

[17] T. Taha, Z.F. Cui, CFD modelling of slug flow in vertical tubes, *Chem. Eng. Sci.* 61 (2006) 676-687.

[18] A.N. Asadolahi, R. Gupta, D.F. Fletcher, B.S. Haynes, CFD approaches for the simulation of hydrodynamics and heat transfer in Taylor flow, *Chem. Eng. Sci.* 66 (2011) 5575-5584.

[19] A.N. Asadolahi, R. Gupta, S.S.Y. Leung, D.F. Fletcher, B.S. Haynes, Validation of a CFD model of Taylor flow hydrodynamics and heat transfer, *Chem. Eng. Sci.* 69 (2012) 541-552.

[20] D. Zheng, M. He, D. Che, CFD simulations of hydrodynamic characteristics in a gas-liquid vertical upward slug flow, *Int. J. Heat Mass Transfer.* 50 (2007) 4151-4165.

[21] R. Kaya, G. Deveci, T. Turken, R. Sengur, S. Guclu, D. Y. Koseoglu-Imer, I. Koyuncu, Analysis of wall shear stress on the outside-in type hollow fiber membrane modules by CFD simulation, *Desalination.* 351 (2014) 109-119.

[22] L. Zhuang, H. Guo, G. Dai, Z. Xu, Effect of the inlet manifold on the performance of a hollow fiber membrane module-A CFD study, *J. Membrane. Sci.* 526 (2017) 73-93.

[23] K. B. Lim, P. C. Wang, H. An, S. C. M. Yu, Computational Studies for the Design Parameters of Hollow Fibre Membrane Modules, *J. Membrane. Sci.* 529 (2017) 263-273.

[24] X. Yang, H. Yu, R. Wang, A. G. Fane, Optimization of microstructured hollow fiber design for membrane distillation applications using CFD modeling. *J. Membrane. Sci.* 421-422 (2012) 258-270.

[25] K. Essemiani, G. Ducom, C. Cabassud, A. Liné, Spherical cap bubbles in a flat sheet nanofiltration module: experiments and numerical simulation, *Chem. Eng. Sci.* 56 (2001) 6321-6327.

[26] S. M. Javid, M. Passandideh-Fard, A. Faezian, M. Goharimanesh. Slug and bubble flows in a flat sheet ultrafiltration module: Experiments and numerical simulation, *Int. J. Multiphas. Flow.* 91 (2017) 39-50.

[27] C W Hirt, B D Nichols. Volume of fluid (VOF) method for the dynamics of free boundaries. *J. Comput. Phys.* 1981; 39: 201-225.

[28] T H Shih, W W Liou, A Shabbir, Z Yang, J Zhu. A new Kappa-Epsilon eddy viscosity model for high Reynolds-number turbulent flows. *Comput. Fluids.* 1995; 24: 227-238.

[29] Reynolds W C. Fundamentals of turbulence for turbulence modeling and simulation. Lecture Notes for Von Karman Institute, 1987, Agard Report No. 755.

[30] FLUENT 17.0 Theory Guide (2017), ANSYS, Inc., Pennsylvania.

[xx] <http://www.oxiamem.com>